# Analysis of flexible anchored quay walls

Mohamed E. El-Naggar
*Civil Engineering Department, Faculty of Engineering, Alexandria University, Egypt*

Anchored retaining walls are one of a quite complex type of geotechnical structures, which is not only supported by the soil but also loaded by the soil. This paper describes the development of design method used in the analysis of this type of walls. It deals with the use of sub-grade reaction method to the design and analysis of the wall. The contribution of finite element method in this field is used herein to determine the lateral movements, the bending moments of the wall, the passive earth pressure of the soil and the tensile force exerted by the anchor rods.

تستخدم حوائط الارصفة ذات المرابط الخلفية لرسو السفن بانواعها المختلفة وذلك لشحن وتفريغ البضائع أو الركاب مما يتطلب دراسة هذه المنشآت بعناية للتأكد من أتزانها نتيجة القوي المؤثرة عليها والناتجة من تأثير الأوناش أو الشد علي مدافع الرباط أو الصدمات أو نتيجة للضغوط الجانبية للتربة. ويهدف هذا البحث إلى دارسة وتحليل هذا النوع من الحوائط وتحديد العوامل المختلفة والتي تؤثر علي تصميمها وذلك بهدف زيادة اتزانها وتقليل الازاحات الأفقية لها ومن ثم تحديد القوي الداخلية للحائط والشد علي المرابط الخلفية. ولتحديد تاثير العوامل المختلفة والمؤثرة علي اتزان الحائط فقد تم استخدام نظرية العناصر المحددة لدراسة كل عامل علي حده ومن ثم تحديد تأثير كل العوامل مجتمعة. وقد أوضحت الدراسة انه كلما زادت جساءة الحائط واستخدام تربة ردم متماسكة خلفه قلت الحركة الافقية والعزوم الداخلية للحائط وقوي الشد المتولده في المرابط الخلفية وكذلك الضغوط السالبة للتربة وقد تم استنتاج معادلات نظرية لتحديد تلك القوي نتيجة لتاثير كل العوامل مجتمعة.

**Keywords:** Anchored retaining walls, Anchor rod, Earth pressure, Marine quay walls, Penetration depth

## 1. Introduction

Anchored retaining walls are a class of geotechnical structures whose design is governed by the earth pressure imposed by the soil. These structures are widely used in many types of civil engineering construction, particularly in waterfront structures. They are used to hold or prevent the backfill from sliding while may also provide protection against light-to-moderate wave action. They are also used for reclamation projects, where a fill is needed seaward of the existing shore and for marinas and other structures where deep water is needed directly at the shore. Fig. 1 illustrates the main components of the anchored retaining walls.

The analysis and design of this type of walls requires a good knowledge of the soil and water pressure, where they will be exerted. Anchored retaining walls have the ability to deform, so it can be considered as flexible structures, [1,2,3]. The analysis and design of flexible retaining walls has been carried out assuming limit pressures. The first one is the pressure acting upon the inner face of the wall including the active earth pressure produced by the backfill weight, the lateral pressure due to the effect of line and/or uniform distributed loads applied at the surface, and the lateral pressure resulting from the unbalanced water pressure. The second is the pressure affected on the front of the wall; embedment below the dredge line provides passive resistance against an outward movement of the buried part of the wall. Fig. 2 shows the distribution of active and passive earth pressures resisted on anchored retaining walls driven into granular soils.

The depth of penetration is the solution key of any sheet-pile wall. In order to determine the penetration depth, moments are taken about the point of connection between the anchor and the wall. Empirical rules are used to determine the bending moments and the shear forces exerted in the wall, and the tensile force exerted in the anchor. While this is usually adequate to determine the necessary penetration, the empirical methods of analysis are often unreliable for predicting bending moments of the wall and soil-


© Faculty of Engineering Alexandria University, Egypt.

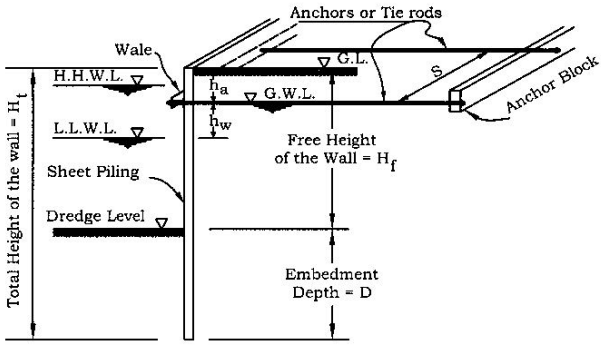


Fig. 1. Anchor sheet pile wall.

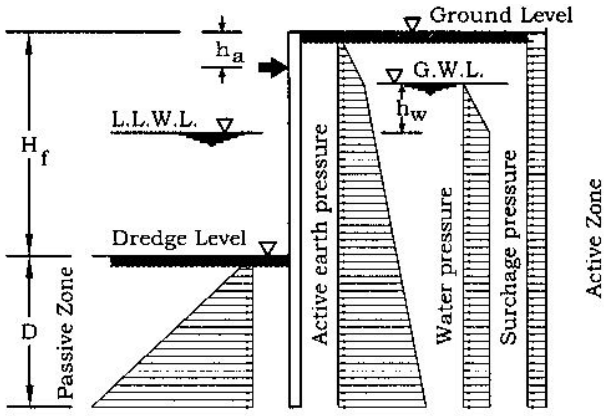


Fig. 2. Distribution of active and passive earth pressures on an anchored retainig wall.

structure interaction. The wall movements, bending moments and shear forces are greatly dependent on the stiffness of the wall, anchor and the soil.

To investigate the behavior of flexible anchored retaining walls and to predict wall movements, the method of beam on elastic foundation was used. Finite element method has been employed for the analysis of practical retaining wall problems. The issues that must be considered is developing such models include modeling of wall and anchor stiffness, and the modeling of sub-grade reaction of the soil.

This paper describes the development of such model and demonstrates its performance as a design tool under practical conditions. Parametric studies, which affect the performance of the anchored quay walls, were considered as design parameters.

## 2. Soil- modeling

### *2.1. Sub-grade reaction method*

The behavior of the soil can be represented by linear elastic springs connected to the wall at node points in the passive region under the dredge line in the front of the wall. Bowles [4] has shown that this model is reasonably correct by using it to analyze full-scale field walls and for reanalyzing model sheet pile walls reported by Tschebotarioff [5] and by Rowe [6]. The sub-grade reaction method is relatively easy to implement in the finite element model. Springs to match the soil response are used to represent the soil modeling. The modulus of sub-grade reaction, $k_s$ is a conceptual relation between the ultimate bearing capacity of the soil, $q_{ult}$ and the soil deflection, $\Delta$ which can be obtained as:

$$ks = qult / \Delta, \quad (1)$$

in which: $k_s$ is the modulus of sub-grade reaction, $q_{ult}$ is ultimate bearing capacity of the soil, and $\Delta$ is the soil deflection.

The numerical value of $k_s$ is very difficult to estimate. After a series of experimental tests, Terzaghi [7] suggested that the horizontal or vertical modulus of sub-grade reaction, $k_s$ could be estimated from:

$$k_S = As + Bs\, Z^n, \quad (2)$$

where, As is a constant for either horizontal or vertical members, *Bs* is a coefficient for depth, *Z* is the depth of interest below ground, and *n* is an exponent to give $k_s$ the best fit. Terzaghi suggested that the value of the exponent, *n* equals one if there is no available data from load-test.

By using the bearing capacity equation, the modulus of sub-grade reaction, $k_s$ for sheet pile walls can be rewritten as:

$$ks = qult / \Delta = C\,(c\,Nc + \gamma\, Z\, N\gamma + 0.5\,\gamma\, B\, Ng), \quad (3)$$

in which: *C* is a factor dependent on the settlement, Bowles [8] showed that $q_{ult}$ occurs at a 1-in or 0.0254-m settlement with no safety factor gives *C* equals 12 or 40, *c* is the

soil cohesion, $N_c$, $N_g$, and $N_\gamma$ are Terzaghi's bearing capacity factors of the soil, $\gamma$ is the unit weight of soil, and, $B$ is the wall width.

Based on eqs. (1) and (3) the two terms of eq. (2) can be written as:

$$As = C\,(c\,Nc + 0.5\,\gamma\,B\,Ng)\,, \tag{4}$$

and

$$Bs\,Z^n = C\,(\gamma\,Z^1\,N\gamma)\,. \tag{5}$$

The previous equations show that the modulus of sub-grade reaction, $k_s$ based on the ultimate bearing pressure at any depth of the wall. Bowles [5] said that the above value of $k_s$ will give reasonable values for bending moment and node soil pressure but deflections, particularly at the dredge line, may be in some error as they are directly dependent on the $k_s$. To overcome this problem, Bowles recommended that the deflection at any node must be limited to a maximum value of deflection; $\Delta_{max}$ when the deflection, $\Delta$ at any node increase than this limit the finite element program will remove the node springs at this node and replace it with a constant negative node force computed as:

$$-Pi = \Delta max\,ksi\,, \tag{6}$$

in which: $k_{si}$ is the node soil spring at node (i), and $P_i$ is the corresponding reversed load at node $i$.

*2.2. Anchor rods and wall modeling*

Anchor rods are modeled as springs applied at the connecting nodes with the sheet pile wall and are characterized with spring stiffness. The stiffness of anchor rod depends on its cross-section area, $A$, modulus of elasticity, $E$, and its length, $L$. The anchor stiffness, $k_{an}$ can be computed as:

$$kan = (A\,E)/L\,. \tag{7}$$

Since the analysis will consider a unit width of the wall, the anchor stiffness is prorated based on the anchor rod spacing, $S$ to obtain the equivalent spring stiffness, $K_{ae}$ as:

$$kae = (A\,E)/(L\,S)\,. \tag{8}$$

To introduce the horizontal effect of the inclined anchors, eq. (8) must be written as:

$$kae = [(A\,E)/(L\,S)]\cos\beta\,, \tag{9}$$

where: $\beta$ is the anchor inclination with the horizontal.

Sheet pile Wall is modeled as a series of elastic beam elements. The stiffness of the wall, $K_w$ is derived using the conventional methods from slope deflection equations. Fig. 3 illustrates the two-dimensional finite element model adopted throughout this analysis. The results from the finite element models are verified with the results obtained by Bowles [8] and a good agreement was found.

## 3. Material properties

The soils used in this study are Well-graded coarse-grained soils compacted to a minimum of 95% standard Proctor density.

The dry and submerged unit weights, ($\gamma_d$ and $\gamma_{sub}$) of these soils are taken to be equal 18.0 and 9.00 kN/m$^3$, respectively, and the angle of internal friction, $\phi$, is taken to be ranged from 25$^o$ to 40$^o$.

The cross-sectional area, $A$, the modulus of elasticity, $E_s$, and the allowable and yield stresses, $f_a$, $f_y$, respectively, define the mechanical properties of the steel anchors used herein. As the analysis will be considered a unit width of the wall, the cross-sectional area of anchor, $A$, is prorated based on the anchor horizontal spacing, $S$. The allowable and yield stresses, $f_a$, $f_y$ of anchor rods are 140 MPa and 280 MPa, respectively, and their modulus of elasticity is 2.0x10$^5$ MPa.

The sheet pile wall is represented in this analysis by its stiffness, $E_sI$, where $E_s$ is the modulus of elasticity and $I$ is the modulus of inertia per meter width of the steel sheet pile.

## 4. Results

*4.1. Lateral movements*

Fig. 4 shows the results of lateral movements' ratio, $\Delta H_f$ of the anchored sheet pile walls of different stiffness, $E_sI$. Seven

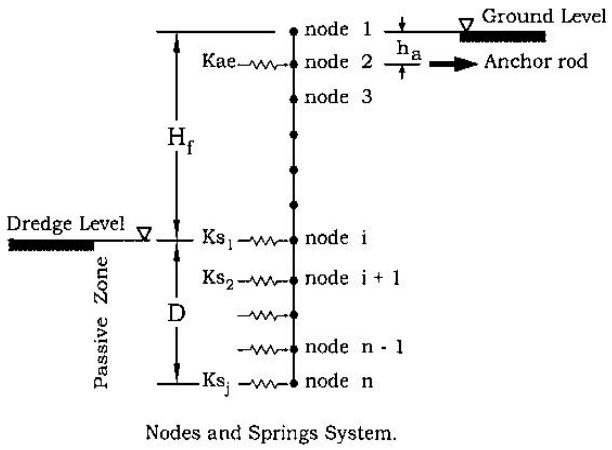


Fig. 3. Finite element model for anchored sheet pile wall.

values of wall stiffness, $E_sI$, which ranged from low to high wall stiffness, were examined. The results show that when the stiffness of the wall increases, the lateral movement ratio, $\Delta H_f$ of the sheet pile wall significantly decreases. The results of very low wall stiffness show unacceptable wall movements, $E_sI = 3*10^3$ and $6*10^3$ kN. m$^2$ while the others show an acceptable movement. The reduction was about 127, 78, 50 and 18% as the wall stiffness, $E_sI$ changed from 12, 18, 24, 36 to $48*10^4$ kN. m$^2$ under the same loading. This reduction occurred due to the contribution of anchored wall stiffness, which helps to increase the over whole stiffness of the structure and thus decrease the lateral movements induced in the anchored wall system. The results also, show that the maximum lateral movements happened approximately, at the same point for different wall stiffness, approximately at O.65 of the free height of the wall, $H_f$. As well as, the displacements at the anchored level and the dredge line significantly reduced as the wall stiffness increase.

The effect of horizontal load in the wall movement under different values of $E_sI$ is illustrated in fig. 5. The results showed a very little reduction of the lateral movement ratio, $\Delta/H_f$ of the wall due to the effect of horizontal force. This reduction could be expected since the direction of lateral load helps the wall to deflect in a direction versus to the deflections due to the effect of the other lateral loads.

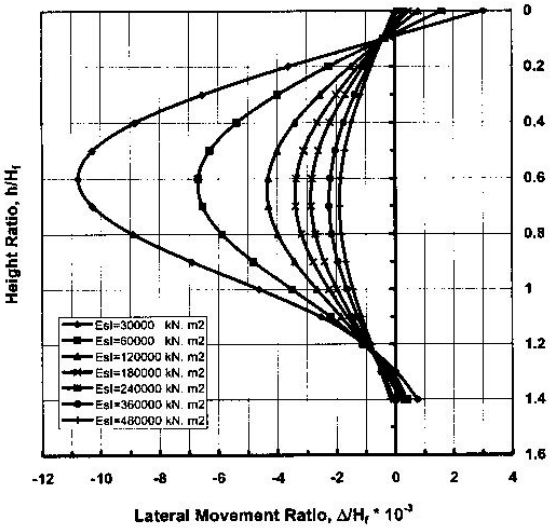


Fig. 4. Lateral $\Delta/H_f$ versus wall stiffness, $E_sI$ of sheet pile wall. ($D/H_f$= 0.4, $h_s/H_f$ = 0.10, $h_w/H_f$=0.10, $\phi$=30$^o$, $\delta$=0.0, $p_v$ = 10 kN/m$^2$).

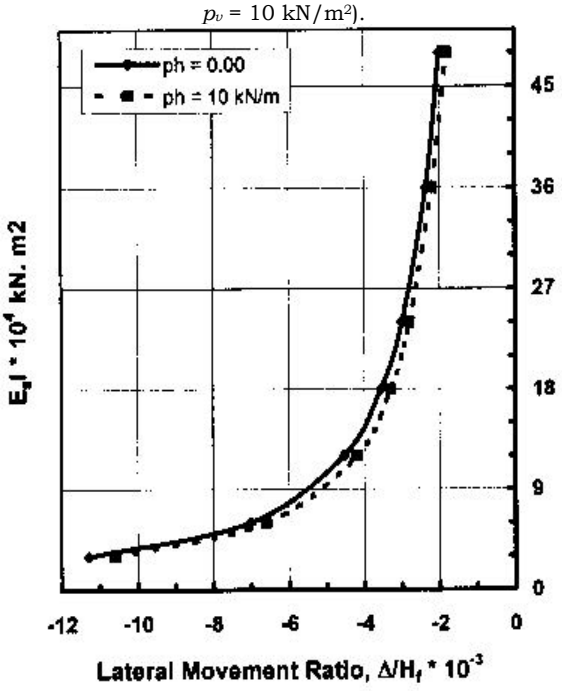


Fig. 5. Maximum lateral movements ratio, $\Delta/H_f$ versus wall stiffness, $E_sI$. ($D/H_f$= 0.4, $h_s/H_f$ = 0.10, $h_w/H_f$=0.10, $\phi$=30$^o$, $\delta$=0.0, $p_v$ = 10 kN/m$^2$).

### *4.2. Bending moments*

Fig. 6 presents the distribution of bending moments along the height of the anchored sheet pile wall under different values of $E_sI$. Excluding the results from walls of low

stiffness, the plots show an increase in the maximum bending moments happened in the free height of the wall when the wall stiffness, $E_sI$ increases. For example, that increase was about 5.5, 13.5 and 20% as the wall stiffness, $E_sI$, changed from 18 to 24, 36 and 48*10$^4$ kN.m$^2$, respectively. In addition, from this figure, we can see that the position of the maximum bending moment occurs, approximately, at the same distance from the dredge level. It happened at a point very close to the point at which the maximum lateral movement occurred, approximately at 0.65 $H_f$. Moreover, the results showed that a significant reduction in the maximum bending moments exerted in the embedded portion of the wall. It is reduced by 43, 74 and 90% as the wall stiffness, $E_sI$ changed from 18 to 24, 36 and 48*10$^4$ kN.m$^2$, respectively. This means that an increase of the wall stiffness, $E_sI$ leads to increase of the rigidity of the structure, which forces the wall to bend to the free height, and thus increases the bending moment toward the free height and reduces it in the embedded portion of the wall.

Fig. 7 illustrates the effect of horizontal load in the maximum bending moments exerted in the anchored sheet pile wall under

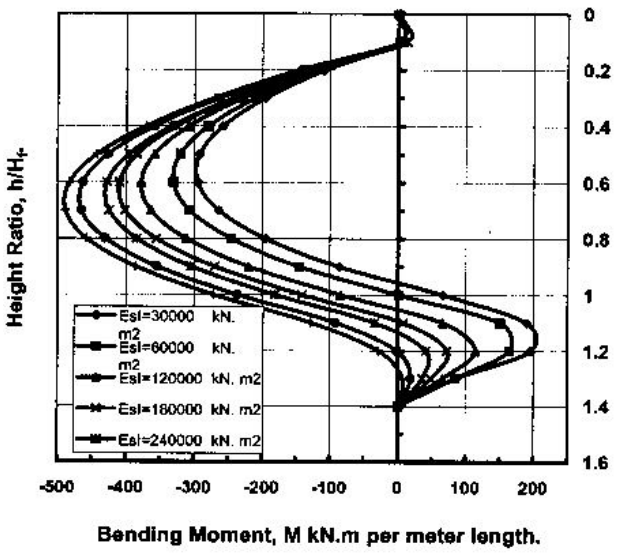


Fig. 6. Bending moments distribution along the anchored wall height. ($D/H_f$= 0.4, $h_s/H_f$ = 0.10, $h_w/H_f$=0.10, $\phi$=30$^o$, $\delta$=0.0, $p_v$ = 10 kN/m$^2$, $p_h$ =0.00).

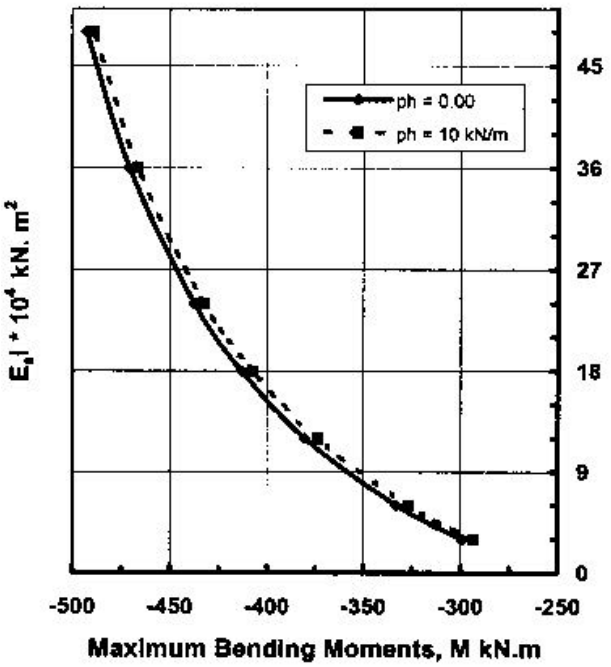


Fig. 7. Maximum bending moments verus wall stiffness, $E_sI$. ($D/H_f$= 0.4, $h_s/H_f$ = 0.10, $h_w/H_f$=0.10, $\phi$=30$^o$, $\delta$=0.0, $p_v$ = 10 kN/m$^2$).

different values of $E_sI$. The results showed a reduction in the maximum bending moment due to the effect of the horizontal force. This reduction could be expected since the lateral load increases the bending moment at the anchored point, which reduces the maximum bending moment exerted in the free height of the wall by this value.

### *4.3. Anchored tensile force*

Fig. 8 presents the maximum anchor force for different anchored wall stiffness, $E_sI$. It can be seen that the walls of low stiffness, $E_sI$ carry a smallest value of the anchor load than the walls of high stiffness. In addition, the horizontal load significantly increases the anchor load in all cases of wall stiffness, $E_sI$. The plot in this figure shows, approximately, the same value of increase for all cases of wall stiffness. It is about 7.50% in all wall stiffness. This could be expected since the position of anchor is very close to the point of horizontal load effect.

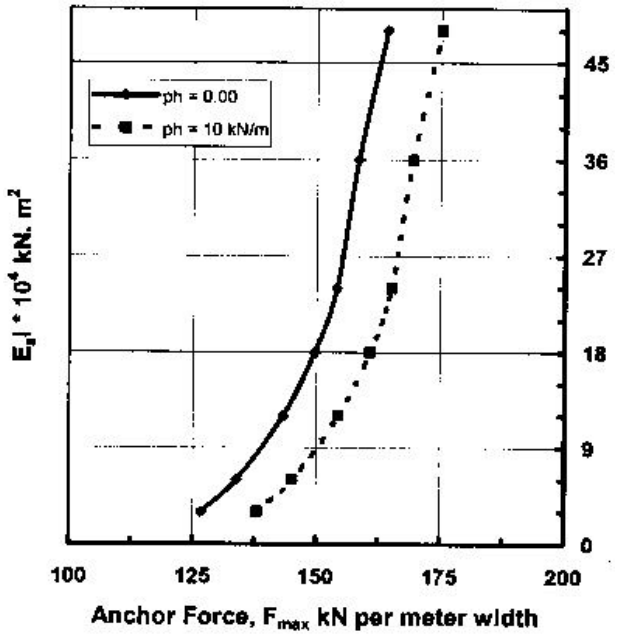


Fig. 8. Maximum anchor force, $F_{max}$ verus wall stiffness, $E_sI$. ($D/H_f$= 0.4, $h_s/H_f$ = 0.10, $h_w/H_f$=0.10, $\phi$=30°, $\delta$=0.0, $p_v$ = 10 kN/m$^2$).

*4.4. Passive earth pressure*

The results showed that the use of high stiffness walls has an important role in improving the distribution of the passive earth pressure. The distribution of passive earth pressure is very close to be a uniform distribution for high stiffness walls, fig. 9. The position of the maximum passive earth pressure is varying according to the stiffness of the wall. It occurred, approximately, at 0.10 $H_f$ (about quarter the embedded depth, $D$) and 0.20 $H_f$ (about half the embedded depth, $D$), from the dredge line, for low and high wall stiffness, respectively. In addition, the results show a reduction in the maximum passive earth pressure as the wall stiffness, $E_sI$, increase. It was reduced by 22, 15 and 6% as the wall stiffness, $E_sI$ changed from 18, 24, 36 to 48*10$^4$ kN.m$^2$, respectively.

## 5. Parameters of analysis

Fig. 1 illustrates the geometry of the anchored retaining wall system. The parameters considered in the analysis are including the following:

i. Wall stiffness, in terms of ($E_sI$);
ii. Vertical applied Load, $p_v$;
iii. Horizontal load, $p_h$;
iv. Water height ratio, $h_w/H_f$;
v. Anchor Location, $h_a$, in terms of $h_a/H_f$;
vi. Wall-soil angle of friction between, $\Delta$;
vii. Angle of internal friction of backfill soil, $\phi$; and,
viii. Penetration depth ratio, $D/H_f$.

*5.1. Wall stiffness, $E_sI$ as a variable*

As mentioned before, wall stiffness, $E_sI$ has a great role in the analysis of the anchored sheet pile walls. To determine this role, four values of wall stiffness, $E_sI$ were adopted, $E_sI$ = 18 to 24, 36 and 48*10$^4$ kN.m$^2$). The other parameters of the model were considered constant as, $D/H_f$=0.40, $h_a/H_f$=0.10, $h_w/H_f$ =0.10, $\phi$=30°, $\delta$=0.0, $p_v$=10 kN/m$^2$, and $p_h$=0.00. The results obtained from models of different wall stiffness showed that the lateral movements, the bending moments of the wall, the passive earth pressure and the tensile forces exerted by the anchor rod are highly dependent on the wall stiffness, $E_sI$.

*5.1.1. Maximum lateral movement ratio, $(\Delta/H_f)_{EI}$*

Fig. 10 represents the variation of the lateral movement ratio, $(\Delta/H_f)_{EI}$, due to different wall stiffness, $E_sI$. The results show a linear trend when $ln(E_sI)$ is plotted versus the maximum lateral movement ratio, $(\Delta/H_f)_{EI}$. From the best fit of the plot in fig. 10, the maximum lateral movement ratio, $(\Delta/H_f)_{EI}$ may be approximately given as the following:

$$\left(\frac{\Delta}{H_f}\right)_{EI} = \frac{1}{656}\left(14.30 - ln(E_sI)\right), \qquad (10)$$

where: $(\Delta/H_f)_{EI}$ is the maximum lateral movement ratio due to the effect of different wall stiffness, $E_sI$.

*5.1.3. Maximum bending moments, $M_{EI}$*

Fig. 11 illustrates the relationship between the maximum bending moments, $M_{EI}$ and the wall stiffness, $E_sI$. The results show a linear relationship on semi-logarithmic scale. Based on the plotted results in fig. 11, the maximum

bending moment, $M_{EI}$ can be approximately expressed as:

$$M_{EI}= \frac{163}{2}\left[ln\,(E_sI) - 7.03\right], \qquad (11)$$

in which: $M_{EI}$ is the maximum bending moment in the anchor wall in kN.m per meter width of the wall.

*5.1.3. Maximum anchor tensile force, $F_{EI}$*

The role of wall stiffness, $E_sI$, in the effect of the maximum anchor tensile force, $F_{EI}$ is dem onstrated in fig. 12. From the best fit of this plot, the maximum anchor tensile force, $F_{EI}$ may be approximately given by:

$$F_{EI}= \frac{149}{10}\left[ln\,(E_sI) - 2.00\right]. \qquad (12)$$

in which: $F_{EI}$ is the maximum anchor tensile force in kN per meter width of the wall.

*5.1.4. Maximum passive earth pressure, $p_{pEI}$*

Fig. 13 presents the relationship between the maximum passive earth pressure, $p_{pEI}$ and the wall stiffness, $E_sI$. The results showed a linear relationship on semi-logarithmic scale. From the best fit of the plot in fig. 13, the maximum passive earth Pressure, $p_{pEI}$ may be given as:

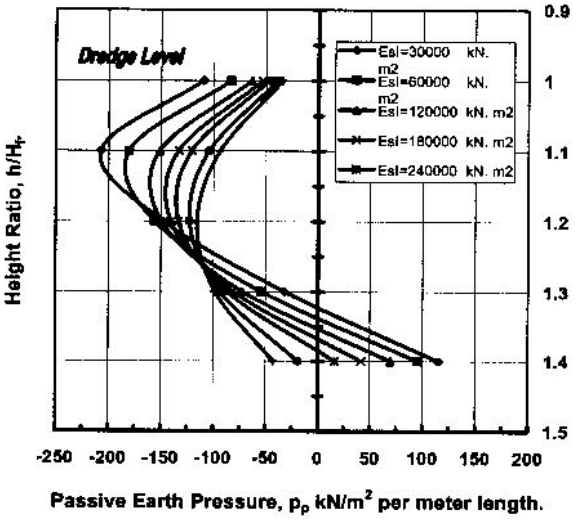


Fig. 9. Passive earth pressure distribution along the embedded height of the wall. ($D/H_f$= 0.4, $h_s/H_f$ = 0.10, $h_w/H_f$=0.10, $\phi$=30°, δ=0.0, $p_v$ = 0.00).

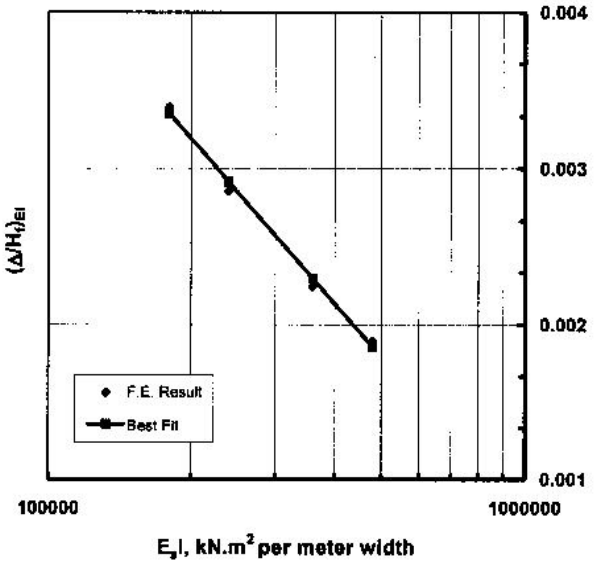


Fig. 10. Maximum lateral movements ratio, $(\Delta/H_f)_{EI}$ versus wall stiffness, $E_sI$. ($D/H_f$= 0.4, $h_s/H_f$ = 0.10, $h_w/H_f$=0.10, $\phi$=30°, $\delta$=0.0, $p_v$ = 10, $pv$ = 10kN/m², $p_h$=0.0).

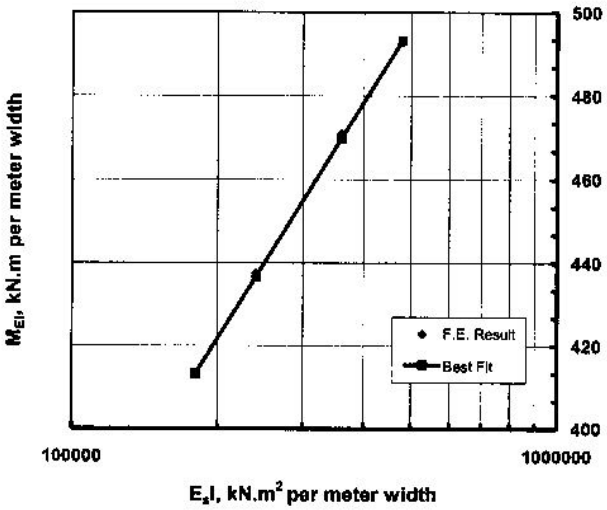


Fig. 11. Maximum bending moments, $M_{EI}$ versus wall stiffness, $E_sI$. ($D/H_f$= 0.4, $h_s/H_f$ = 0.10, $h_w/H_f$=0.10, $\phi$=30°, $\delta$=0.0, $p_v$ = 10, $pv$ = 10kN/m², $p_h$=0.0).

$$p_{pEI}= \frac{51}{2}\left[17.62 - ln\,(E_sI)\right], \qquad (13)$$

in which: $p_{pEI}$ is the maximum passive earth Pressure in kN/m² per meter width of the wall.

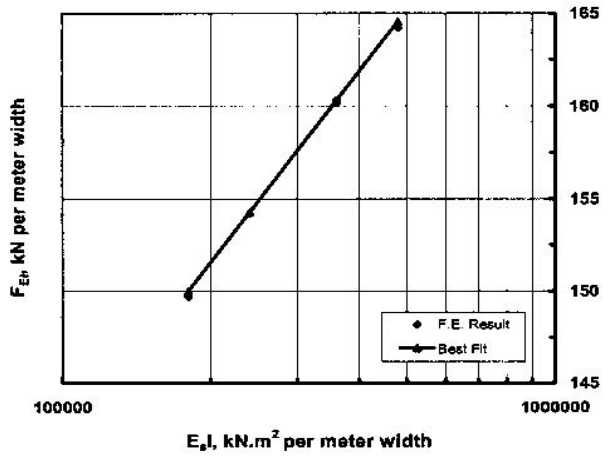


Fig. 12. Maximum Anchor tensile force, $F_{EI}$ versus wall stiffness, $E_sI$. ($D/H_f$= 0.4, $h_s/H_f$ = 0.10, $h_w/H_f$=0.10, $\phi$=30°, $\delta$=0.0, $p_v$ = 10, $pv$ = 10kN/m$^2$, $p_h$=0.0).

*5.2. Vertical load, $p_v$ as a variable*

In this work, four cases of vertical applied loads were conducted, ($p_v$ = 10, 20, 30 and 40 kN/m$^2$). The other variables of the anchored wall system were considered constant as, $D/H_f$=0.40, $h_a/H_f$=0.10, $\phi$=30°, $\delta$=0.0, $E_sI$=4.8*10$^5$ kN.m$^2$/m, and; $p_h$=0.0, respectively. The lateral movements, the bending moments of the wall, the passive earth pressure and the tensile forces exerted by the anchor rod showed a linear relationship when the vertical applied load, $p_v$ plotted against them.

*5.2.1. Maximum lateral movement ratio, $(\Delta/H_f)_{pv}$*

From the best fit of the results, the maximum lateral movement ratio, $(\Delta/H_f)_{pv}$ may be approximately given as the following:

$$\left(\frac{\Delta}{H_f}\right)_{pv} = \frac{1}{656}\left(14.20 - \ln(E_sI) + 0.012\ p_v\right), \quad (14)$$

where: $(\Delta/H_f)_{pv}$ is the maximum lateral movement ratio due to the effect of vertical applied load and $p_v$ is the vertical applied load in kN/m$^2$.

*5.2.2. Maximum bending moments, $M_{pv}$*

Based on the obtained results, the maximum bending moment, $M_{pv}$ can be approximately expressed as:

$$M_{pv} = \frac{163}{2}\left[\ln(E_sI) + 0.055\ p_v - 7.60\right], \quad (15)$$

in which, $M_{pv}$ is the maximum bending moment in the wall in kN.m per meter width of the wall due to the effect of vertical applied load.

*5.2.3. Maximum anchor tensile force, $F_{pv}$*

The maximum anchor tensile force, $F_{pv}$ due to the effect of vertical applied load may be approximately given as the following:

$$F_{pv} = \frac{149}{10}\left[\ln(E_sI) + 0.14\ p_v - 3.60\right], \quad (16)$$

in which: ($F_{pv}$) is the maximum anchor tensile force due to the effect of vertical applied load in kN per meter width of the wall.

*5.2.4. Maximum passive earth pressure, $p_{pv}$*

As well as, the maximum passive earth Pressure, $p_{pv}$ may be approximately expressed as:

$$p_{pv} = \frac{51}{2}\left[17.25 - \ln(E_sI) + 0.036\ p_v\right], \quad (17)$$

in which: $p_{pv}$ is the maximum passive earth pressure due to the effect of vertical applied load in kN/m$^2$ per meter width of the wall.

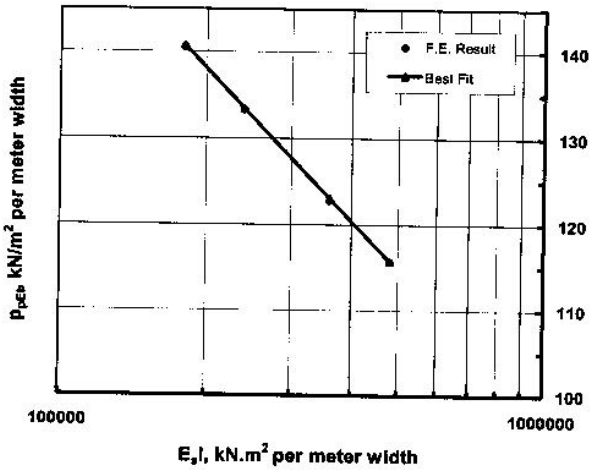


Fig. 13. Maximum passive earth pressure, $p_{PEI}$ versus wall stiffness, $E_sI$. ($D/H_f$= 0.4, $h_s/H_f$ = 0.10, $h_w/H_f$=0.10, $\phi$=30°, $\delta$=0.0, $p_v$ = 10, $pv$ = 10kN/m$^2$, $p_h$=0.0).

*5.3. Horizontal load, $p_h$ as a variable*

As mentioned before, the horizontal load increases the anchor tensile force and reduces the other internal forces of the anchored sheet-pile wall system. Since the critical case of design of any civil engineering structure is the case produced the maximum internal forces, so the horizontal load will use in this work to find the maximum anchor tensile force. For this reason, four cases of horizontal applied loads were conducted, ($p_h$ = 10, 20, 30 and 40 kN per meter width of the wall). The other variables were considered constant as, $D/H_f$=0.40, $h_a/H_f$=0.10, $h_w/H_f$=0.10, $\phi$=30°, $\delta$=0.0, $E_sI$=4.8*10$^5$ kN.m$^2$/m, and; $p_v$=0.0, respectively.

*5.3.1. Maximum anchor tensile force, $F_{ph}$*

The maximum anchor tensile force, $F_{ph}$ due to the effect of horizontal load may be approximately given from:

$$F_{ph} = \frac{149}{10}\left[ln\,(E_sI) + 0.14\ p_v + 0.075\ p_h - 3.80\right], \quad (18)$$

in which, $F_{ph}$ is the maximum anchor tensile force due to the effect of horizontal load in kN per meter width of the wall.

*5.4. Water height ratio, $h_w/H_f$ as a variable*

To examine the effect of water difference in front and back of the structure, four values of $h_w/H_f$ were considered, ($h_w/H_f$ = 0.1, 0.2, 0.3 and 0.4). In all models, the water level in front of the anchored sheet pile wall is considered under the ground level by one meter as recommended in marine platforms. The results show a linear relationship for the maximum lateral movement, the maximum bending moment and the maximum passive earth pressure, and a linear relationship on semi-logarithmic scale for the maximum anchor force, when ($D/H_f$=0.40, $h_a/H_f$=0.10, $\phi$=30°, $\delta$=0.0, $E_sI$=4.8*10$^5$ kN.m$^2$/m, $p_v$=10.00 kN/m$^2$, $p_h$=0.00).

*5.4.1. Maximum lateral movement ratio, $(\Delta/H_f)_w$*

From the best fit of the results, the maximum lateral movement ratio, $(\Delta/H_f)_w$ may be approximately given as the following:

$$\left(\frac{\Delta}{H_f}\right)_w = \frac{1}{656} * \left(13.90 + 0.012p_v - ln(E_sI) + 3.00\ \frac{h_w}{H_f}\right), \quad (19)$$

where: $(\Delta/H_f)_w$ is the maximum lateral movement ratio due to the effect of water difference.

*5.4.2. Maximum bending moments, $M_w$*

Based on the obtained results, the maximum bending moment, $M_w$ can be approximately expressed as:

$$M_w = \frac{163}{2} * \left[ln\,(E_sI) + 0.055\ p_v + 15.35\ \frac{h_w}{H_f} - 9.15\right], \quad (20)$$

in which: $M_w$ is the maximum bending moment in the wall in kN.m per meter width of the wall due to the effect of water difference.

*5.4.3. Maximum anchor tensile force, $F_w$*

From the best fit of the plot in fig. 14, the maximum anchor tensile force, $F_w$ due to the effect of water difference may be approximately given as:

$$F_w = \frac{149}{10}\left[ln\left((E_sI)\left(\frac{h_w}{H_f}\right)^{4.50}\right) + 0.14\ p_v + 0.075\ p_h + 6.55\right], \quad (21)$$

in which: $F_w$ is the maximum anchor tensile force due to the effect of water difference in kN per meter width of the wall.

*5.4.4. Maximum passive earth pressure, $p_{pw}$*

From the best fit of the obtained results, the maximum passive earth Pressure, $p_{pw}$ due to the effect of water difference may be expressed as:

$$p_{pw} = \frac{51}{2}\left[16.25 - ln\,(E_sI) + 0.036\ p_v + 10.10\ \frac{h_w}{H_f}\right], \quad (22)$$

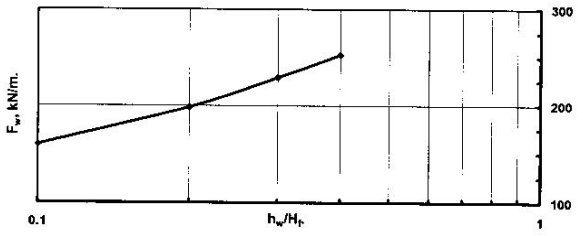


Fig. 14. Water Height, $h_w/H_f$ versus anchor tensile loads, $F_w$ ($D/H_f$= 0.4, $h_s/H_f$ = 0.10, $h_w/H_f$=0.10, $\phi$=30°, $\delta$=0.0, $p_v$ = 10, $pv$ = 10kN/m², $p_h$=0.0).

in which: $p_{pw}$ is the maximum passive earth Pressure due to the effect of water difference in kN/m² per meter width of the wall.

## 6. Anchor position ratio, $h_a/H_f$ as a variable

To determine the contribution of the anchor position ratio, $h_a/H_f$ on the internal forces of the anchored sheet pile system, five values of $h_a/H_f$ were conducted, ($h_a/H_f$ = 0.1, 0.15, 0.2, 0.25 and 0.3). The obtained results show a linear relationship between the anchor position ratio, $h_a/H_f$ and the lateral movements, bending moments of the wall and the passive earth pressure exerted in the soil. Moreover, the variation was linear but on semi-logarithmic scale for the maximum anchor force, when ($D/H_f$=0.40, $h_w/H_f$=0.10, $\phi$=30°, $\delta$=0.0, $E_sI$=4.8*10⁵ kN.m²/m, $p_v$=10 kN/m², $p_h$=0.00).

### 6.1. Maximum lateral movement ratio, $(\Delta/H_f)_a$

From the best fit of the results, the maximum lateral movement ratio, $(\Delta/H_f)_a$ may be approximately given as the following:

$$\left(\frac{\Delta}{H_f}\right)_a = \frac{1}{656}\begin{pmatrix} 14.13 + 0.012p_v - ln(E_sI) \\ + 3.oo\ \frac{h_w}{H_f} - 2.3\frac{h_a}{H_f} \end{pmatrix}, \quad (23)$$

where: $(\Delta/H_f)_a$ is the maximum lateral movement ratio due to the effect of anchor position ratio, $h_a/H_f$.

### 6.2. Maximum bending moments, $M_a$

Based on the obtained results, the maximum bending moment, $M_a$ can be approximately expressed as:

$$M_a = \frac{163}{2}\begin{bmatrix} ln\,(E_sI) + 0.055\ p_v\ + \\ 15.35\ \frac{h_w}{H_f} - 8.9\frac{h_a}{H_f} - 8.20 \end{bmatrix}, \quad (24)$$

in which: $M_a$ is the maximum bending moment in the wall in kN.m per meter width of the wall due to the effect of anchor position ratio, $h_a/H_f$.

### 6.3. Maximum anchor tensile force, $F_a$

From the best fit of the results, the maximum anchor tensile force, $F_a$ due to the effect of anchor position ratio, $h_a/H_f$ may be given from:

$$F_a = \frac{149}{10}\begin{bmatrix} ln\left((E_sI)\left(\frac{h_w}{H_f}\right)^{4.50}\right) + 0.14\ p_v \\ + 0.075\ p_h + 13.90\frac{h_a}{H_f} + 5.20 \end{bmatrix}, \quad (25)$$

in which: $F_a$ is the maximum anchor tensile force due to the effect of anchor position ratio, $h_a/H_f$ in kN per meter width of the wall.

### 6.4. Maximum passive earth pressure, $p_{pa}$

Based on the finite element results, the maximum passive earth Pressure, $p_{pa}$ due to the effect of anchor position ratio, $h_a/H_f$ may be approximately expressed as:

$$p_{pa} = \frac{51}{2}\begin{bmatrix} 16.66 - ln\,(E_sI) + 0.036\ p_v\ + \\ 10.10\ \frac{h_w}{H_f} + 4.10\frac{h_a}{H_f} \end{bmatrix}, \quad (26)$$

in which: $p_{pa}$ is the maximum passive earth Pressure due to the effect of anchor position ratio, $h_a/H_f$ in kN/m² per meter width of the wall.

## 7. Wall-soil angle of friction, $\delta$, as a variable

To represent the contribution of wall-soil angle of friction, $\delta$, on the analysis of anchored sheet pile wall, four values of $\delta$ were adopted, ($\delta$ = 0, 15, 20 and 25). The other variables of

the system were fixed as, ($D/H_f$=0.40, $h_a/H_f$=0.10, $h_w/H_f$=0.10, $\phi$=30°, $p_v$=10 kN/m², $p_h$=0.00).

*7.1. Maximum lateral movement ratio, $(\Delta/H_f)_\delta$*

Fig. 15 represents the variation of the lateral movement ratio, $(\Delta/H_f)_\delta$ due to different values of wall-soil angle of friction, $\delta$. The results showed a linear relationship on semi-logarithmic scale. From the best fit of the plot in fig. 15, the maximum lateral movement ratio, $(\Delta/H_f)_\delta$ may be given from:

$$\left(\frac{\Delta}{H_f}\right)_\delta = \frac{e^{-(\frac{\delta}{276})}}{656}\begin{pmatrix} 14.13 + 0.012p_v - \ln(E_sI) \\ + 3.00\,\frac{h_w}{H_f} - 2.3\,\frac{h_a}{H_f} \end{pmatrix}, \quad (27)$$

where: $(\Delta/H_f)_\delta$ is the maximum lateral movement ratio due to the effect of different wall-soil angle of friction, $\delta$.

*7.2. Maximum bending moments, $M_\delta$*

Fig. 16 illustrates the relation between the maximum bending moments, $M_\delta$ and different values of wall-soil angle of friction, $\delta$. The results show a linear relationship on semi-logarithmic scale. Based on the plot in fig. 16, the maximum bending moment, $M_\delta$ can be expressed as:

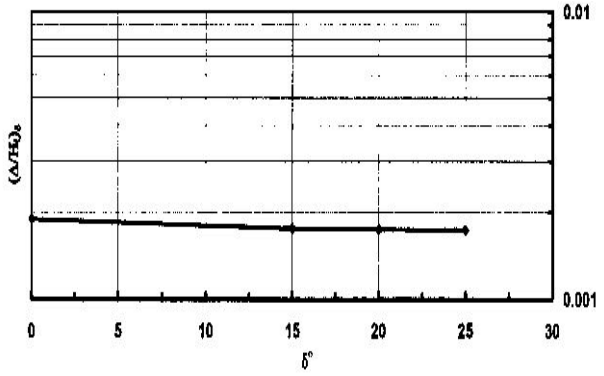


Fig. 15. Wall-soil angle of friction, δ versus maximum lateral movements ratio, $(\Delta/H_f)_\delta$. ($D/H_f$= 0.4, $h_s/H_f$ = 0.10, $h_w/H_f$=0.10, $\phi$=30°, $\delta$=0.0, $p_v$ = 10, $p\upsilon$ = 10kN/m², $p_h$=0.0).

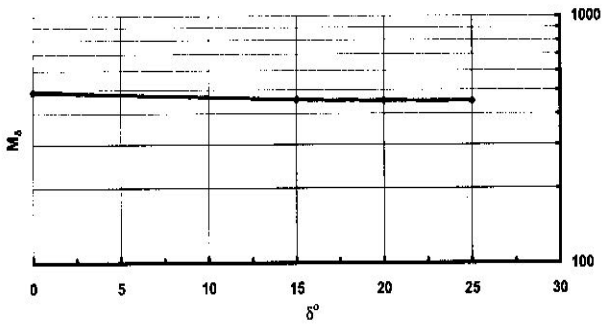


Fig. 16. Wall-soil angle of friction, δ versus maximum bending moments, $M_\delta$. ($D/H_f$= 0.4, $h_s/H_f$ = 0.10, $h_w/H_f$=0.10, $\phi$=30°, $h_w/H_f$= 0.10, $p_v$ = 10.0, kN/m², $E_sI$ =2.4*10⁵ kN.m²/m.)

$$M_\delta = \frac{149}{10\,e^{\frac{\delta}{276}}}\begin{bmatrix} \ln(E_sI) + 0.055\ p_v\ + 15.35\,\frac{h_w}{H_f} \\ -8.9\,\frac{h_a}{H_f} - 8.20 \end{bmatrix}. \quad (28)$$

in which: $M_\delta$ is the maximum bending moment in the sheet pile wall in kN.m per meter width of the wall due to different value of wall-soil angle of friction, $\delta$.

*7.3. Maximum anchor tensile force, $F_\delta$*

Fig. 17 demonstrates the variation between the maximum anchor tensile force, $F_\delta$ and different values of wall-soil angle of friction, $\delta$ From the best fit of this plot, the maximum anchor tensile force, $F_\delta$ may be approximately given as the following:

$$F_\delta = \frac{149}{10\,e^{\frac{\delta}{292}}}\begin{bmatrix} \ln\left((E_sI) * (\frac{h_w}{H_f})^{4.50}\right) + 0.14\ p_v \\ + 0.075\ p_h + 13.90\,\frac{h_a}{H_f} + 5.20 \end{bmatrix} \quad (29)$$

in which: $F_\delta$ is the maximum anchor tensile force in kN per meter width of the wall due to different value of wall-soil angle of friction, $\delta$.

*7.4. Maximum passive earth pressure, $p_{p\delta}$*

Fig. 18 presents the relationship between the maximum passive earth pressure, $p_{p\delta}$ and different values of wall-soil angle of friction, δ. From the best fit of the plot in fig. 18, the maximum passive earth Pressure, $p_{p\delta}$ may be expressed from the following:

$$p_{p\delta} = \frac{51}{2\,e^{\frac{\delta}{266}}}\left[\begin{array}{l} 16.66 - \ln(E_s I) + 0.036\, p_v \\ +10.10\,\frac{h_w}{H_f} + 4.10\,\frac{h_a}{H_f} \end{array}\right] \qquad (30)$$

in which: $p_{p\delta}$ is the maximum passive earth pressure in kN/m$^2$ per meter width of the wall due to different value of wall-soil angle of friction, $\delta$.

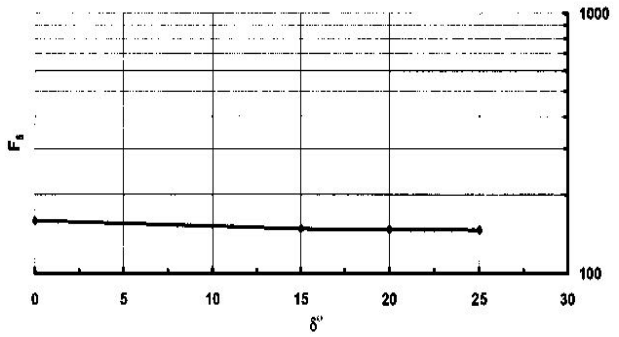


Fig. 17. Wall-soil angle of friction, δ versus maximum anchor tensile force, $\delta$ ($D/H_f$= 0.4, $h_s/H_f$ = 0.10, $h_w/H_f$=0.10, $\phi$=30°, $h_w/H_f$= 0.10, $p_v$ = 10.0, kN/m$^2$, $E_sI$ =2.4*10$^5$ kN.m$^2$/m).

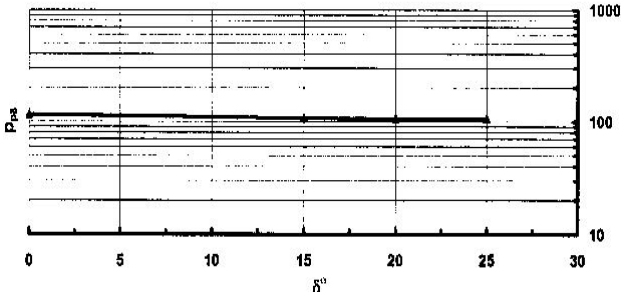


Fig. 18. Wall-soil angle of friction, δ versus maximum passive earth pressure, $p_{p\delta}$. ($D/H_f$= 0.4, $h_s/H_f$ = 0.10, $h_w/H_f$=0.10, $\phi$=30°, $h_w/H_f$= 0.10, $p_v$ = 10.0, kN/m$^2$, $E_sI$ =2.4*10$^5$ kN.m$^2$/m).

## 8. Angle of internal friction of backfill soil, $\phi$, as a variable

To demonstrate the effect of the angle of internal friction of the backfill soil, $\phi$, on the internal forces of the anchored sheet pile system, four values of $\phi$ were considered, ($\phi$ = 25, 30, 35 and 40). The other variables of the system were considered constant as, ($D/H_f$= 0.4, $h_a/H_f$=0.10, $h_w/H_f$=0.10, $\delta$=0.00, $p_v$=10 kN/m$^2$, $p_h$=0.00).

*8.1. Maximum lateral movement ratio, $(\Delta/H_f)_\phi$*

Fig. 19 represents the variation of the lateral movement ratio, $(\Delta/H_f)_\phi$ due to different values of angle of internal friction, $\phi$. The results showed a linear relationship on semi-logarithmic scale. From the best fit of the plot in fig. 19, the maximum lateral movement ratio, $(\Delta/H_f)_\phi$ may be given from:

$$\left(\frac{\Delta}{H_f}\right)_\varphi = \frac{5\,e^{-\left(\frac{\delta}{276}+\frac{5\varphi}{66}\right)}}{337} \left(\begin{array}{l} 14.13 + 0.012 p_v - \ln(E_s I) \\ +3.00\,\frac{h_w}{H_f} - 2.3\,\frac{h_a}{H_f} \end{array}\right), \qquad (31)$$

where: $(\Delta/H_f)_\phi$ is the maximum lateral movement ratio due to the effect of different values of angle of internal friction, $\phi$.

*8.2. Maximum bending moments, $M_\phi$*

Fig. 20 illustrates the relation between the maximum bending moments, $M_\phi$ and different values of angle of internal friction, $\phi$. Based on the plot in this figure, the maximum bending moment, $M_\phi$ can be expressed as:

$$M_\varphi = \frac{421.50}{e^{\left(\frac{\delta}{276}+\frac{\varphi}{18}\right)}}\left[\begin{array}{l} \ln(E_s I) + 0.055\; p_v \; + \\ 15.35\,\frac{h_w}{H_f} - 8.9\,\frac{h_a}{H_f} - 8.20 \end{array}\right] \qquad (32)$$

in which: $M_\phi$ is the maximum bending moment in the sheet pile wall in kN.m per meter width

of the wall due to different value of angle of internal friction, $\phi$.

*8.3. Maximum anchor tensile force, $F_\phi$*

Fig. 21 demonstrates the relationship between the maximum anchor tensile force, $F_\phi$ and different values of angle of internal friction, $\phi$. From the best fit of the plot in fig. 21, the maximum anchor tensile force, $F_\phi$ may be approximately given as the following:

$$F_\varphi = \frac{52.40}{e^{\left(\frac{\delta}{292}+\frac{\varphi}{24}\right)}} \left[ \begin{array}{l} ln\left( (E_s I)\left(\frac{h_w}{H_f}\right)^{4.50} \right) + 0.14\ p_v + \\ 0.075\ p_h + 13.90\frac{h_a}{H_f} + 5.20 \end{array} \right], \quad (33)$$

in which: $F_\phi$ is the maximum anchor tensile force in kN per meter width of the wall due to different value of angle of internal friction, $\phi$

*8.4. Maximum passive earth pressure, $p_{p\phi}$*

Fig. 22 presents the relationship between the maximum passive earth pressure, $p_{p\phi}$ and different values of angle of internal friction, $\phi$. From the best fit of the plot in fig. 22, the maximum passive earth Pressure, $p_{p\phi}$ may be taken from the following:

$$p_{p\varphi} = \frac{32.70}{e^{\left(\frac{\delta}{266}+\frac{\varphi}{120}\right)}} \left[ \begin{array}{l} 16.66 - ln\,(E_s I) + 0.036\ p_v \\ + 10.10\ \frac{h_w}{H_f} + 4.10\frac{h_a}{H_f} \end{array} \right], \quad (34)$$

in which: $p_{p\phi}$ is the maximum passive earth Pressure in kN/m$^2$ per meter width of the wall due to different value of angle of internal friction, $\phi$.

## 9. Penetration depth ratio, $D/H_f$, as a variable

To state the effect of the embedment depth ratio, $D/H_f$, on the internal forces of the anchored sheet pile system, six values of $D/H_f$ were adopted, ($D/H_f$ = 0.30, 0.40, 0.50, 0.60, 0.70 and 0.80). The other variables of the system were considered constant as ($h_a/H_f$ =0.10, $h_w/H_f$=0.10, $\phi$= 30°, $\delta$=0.00, $p_v$=10 kN/m$^2$, $p_h$=0.00).

*9.1. Maximum lateral movement ratio, $(\Delta/H_f)_{max}$*

Fig. 23 represents the variation of the lateral movement ratio, $(\Delta/H_f)_{max}$ due to different values of the embedment depth ratio, $D/H_f$. The results showed a linear relationship on semi-logarithmic scale. From the best fit of the plot in fig. 23, the maximum

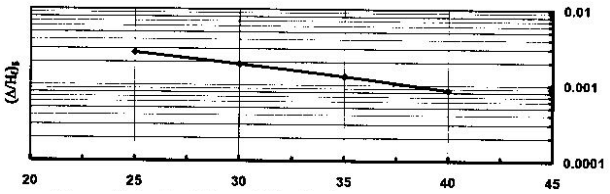


Fig. 19. Angle of internal friction, ϕ versus maximum lateral movements ratio, $(\Delta/H_f)_\phi$. ($D/H_f$= 0.4, $h_s/H_f$ = 0°, $h_w/H_f$=0.10, $p_h$ = 0.0, kN/m$^2$, $E_sI$ =2.4*10$^5$ kN.m$^2$/m).

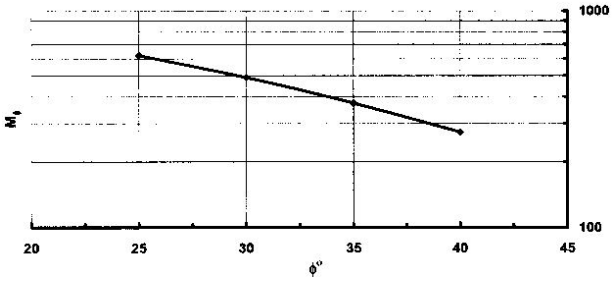


Fig. 20. Angle of internal friction, ϕ versus maximum bending moments, $M_\phi$ ($D/H_f$= 0.4, $h_s/H_f$ = 0.10, $p_h$ = 0.0, kN/m$^2$, $E_sI$ =2.4*10$^5$ kN.m$^2$/m).

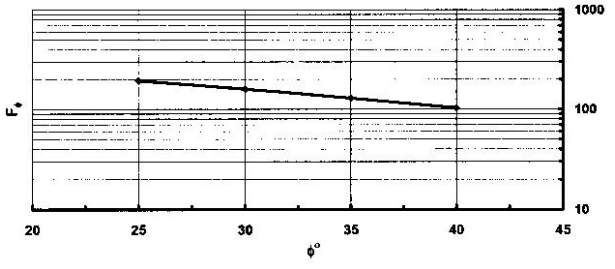


Fig. 21. Angle of internal friction, $\phi$ versus maximum tensile force, $F_\phi$ ($D/H_f$= 0.4, $h_s/H_f$ = 1.0°, $h_w/H_f$=0.10, $p_h$ = 0.0, $p_v$ =10.0 kN/m$^2$, $E_sI$ =2.4*10$^5$ kN.m$^2$/m).

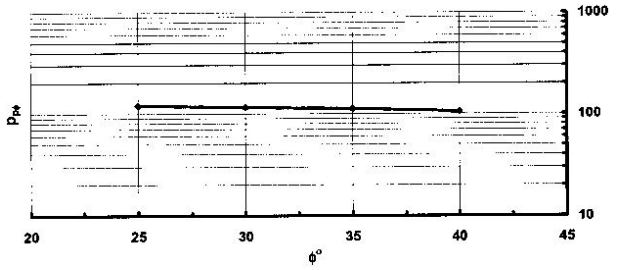


Fig. 22. Angle of internal friction, $\phi$ versus maximum passive earth pressure, $p_{p\phi}$. ($D/H_f$= 0.4, $h_s/H_f$ = 0.1°, $\delta$ =0°, $h_w/H_f$=0.10, $p_h$ = 0.0, kN/m², $E_sI$ =2.4*10⁵ kN.m²/m).

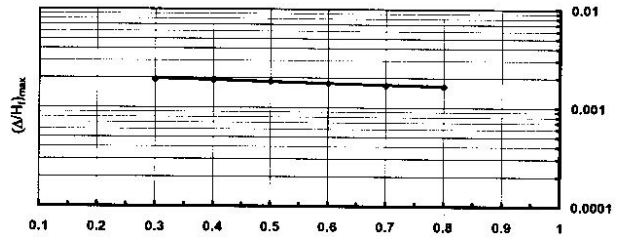


Fig. 23. Embedment depth ratio, $D/H_f$ versus maximum lateral movements ratio, $(\Delta/H_f)_{mzx.}$ ($h_s/H_f$ = 1.0, $\phi$ = 30°, $h_w/H_f$=0.10, $p_h$ = 0.0, $p_v$ = 10.0 kN/m², $E_sI$ =2.4*10⁵ kN.m²/m).

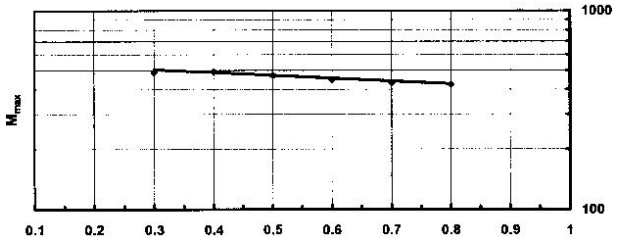


Fig. 24. Embedment depth ratio, $D/H_f$ versus maximum bending moments, $M_{max}$. ($h_s/H_f$ = 30°, $\delta$ =0°, $h_w/H_f$=0.10, $p_h$ = 0.0, $p_v$ = 10.0 kN/m², $E_sI$ =2.4*10⁵ kN.m²/m).

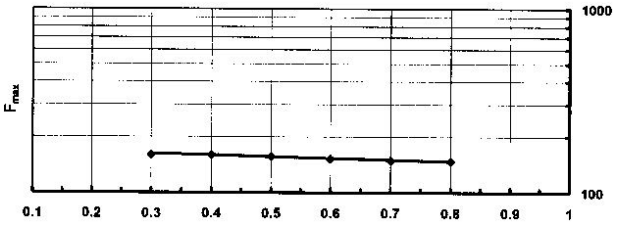


Fig. 25. Embedment depth ratio, $D/H_f$ versus maximum anchor tensile force, $M_{max}$. ($h_s/H_f$ = 30°, $\delta$ =0°, $h_w/H_f$=0.10, $p_h$ = 0.0, $p_v$ = 10.0 kN/m², $E_sI$ =2.4*10⁵ kN.m²/m).

lateral movement ratio, $(\Delta/H_f)_{max}$ may be given from:

$$\left(\frac{\Delta}{H_f}\right)_{max} = \frac{5\,e^{-\left(\frac{\delta}{276}+\frac{5\varphi}{66}+\frac{5\,D}{14\,H_f}\right)}}{292} \left(14.13 + 0.012p_v - \ln(E_sI) + 3\,\frac{h_w}{H_f} - 2.3\,\frac{h_a}{H_f}\right), \quad (35)$$

Where, $(\Delta/H_f)_{max}$ is the maximum lateral movement ratio due to different variables of the anchored wall system.

### 9.2. Maximum bending moments, $M_{max}$

Fig. 24 illustrates the relation between the maximum bending moments, $M_{max}$ and different values of the embedment depth ratio, $D/H_f$. Based on the plot in this figure, the maximum bending moment, $M_{max}$ can be expressed as:

$$M_{max} = \frac{478}{e^{\left(\frac{\delta}{276}+\frac{\varphi}{18}+\frac{D}{3H_f}\right)}} \left[\begin{array}{l} \ln (E_sI) + 0.055\ p_v + 15.35 \\ \frac{h_w}{H_f} - 8.9\,\frac{h_a}{H_f} - 8.20 \end{array}\right], \quad (36)$$

in which, $M_{max}$ is the maximum bending moment in the sheet pile wall in kN.m per meter width due to different variables of the anchored wall system.

### 9.3. Maximum anchor tensile force, $F_{max}$

Fig. 25 demonstrates the relationship between the maximum anchor tensile force, $F_{max}$ and different values of the embedment depth ratio, $D/H_f$. From the best fit of the plot in fig. 25, the maximum anchor tensile force, $F_{max}$ may be approximately given as the following:

$$F_{max} = \frac{56.25}{e^{\left(\frac{\delta}{292}+\frac{\varphi}{24}+\frac{D}{5\,H_f}\right)}}, \left[\begin{array}{l} \ln\left((E_sI)\left(\frac{h_w}{H_f}\right)^{4.50}\right) \\ +\frac{7}{50}\ p_v + \frac{3}{40}\ p_h + 13.9\,\frac{h_a}{H_f} + 5.2 \end{array}\right], \quad (37)$$

in which: $F_{max}$ is the maximum anchor tensile force in kN per meter width due to different variables of the anchored wall system.

*9.4. Maximum passive earth pressure, $p_{pmax}$*

Fig. 26 presents the relationship between the maximum passive earth pressure, $p_{pmax}$ and different values of the embedment depth ratio, $D/H_f$. From the best fit of the plot in the previous figure, the maximum passive earth Pressure, $p_{pmax}$ may be exerted from:

$$p_{pmax} = \frac{34.55}{e^{\left(\frac{\delta}{266}+\frac{\varphi}{120}+\frac{D}{13H_f}\right)}} \left[16.66 - \ln(E_sI) + 0.036\ p_v + 10.10\ \frac{h_w}{H_f} + 4.10\ \frac{h_a}{H_f}\right] \quad (38)$$

in which: $p_{pmax}$ is the maximum passive earth Pressure in kN/m$^2$ per meter width of the wall due to different variables of the anchored wall system.

Eqs. from (35) to (38) are general formulas to evaluate the maximum internal forces within the anchored wall system under vertical and horizontal loads due to different design parameters of the structure.

## 10. Conclusions

Anchored retaining wall is a civil engineering construction used to hold or prevent backfill from sliding as well as providing protection against light-to moderate wave actions. The structure was found to be capable to withstanding high-applied forces if the backfill soil and sheet pile wall had enough stiffness.

The primary aim of this study was to identify the role of parameters affecting the performance of the anchored sheet pile walls. It may be concluded that the resistance of the wall are highly dependent on the stiffness of the sheet pile wall and the backfill soil. The lateral movements, the bending moments of the wall, the passive earth pressure exerted in the soil and the tensile forces exerted by the anchor are significantly reduced with the increase of the wall stiffness. The angle of wall friction and the backfill soil stiffness has a moderate effect to reduce the internal forces of the system. Depth of penetration has the most significant parameter of the performance of the wall. Increasing the penetration depth tends to reduce both the lateral movement and bending moments of the wall and both the passive earth pressure and the tensile force exerted by the anchor tie. The resistance of the wall improves when the horizontal load is used since this load helps to reduce the lateral movements, the bending moments and the passive earth pressure but it increases the anchor tensile force. Results also show that the maximum lateral movement and the maximum bending moments occurred approximately at the same location. It is almost at 0.65 of the free height of the wall measured from the ground level. Furthermore, the position of the maximum passive earth pressure is varying according to the stiffness of the wall. It happened, approximately, at 0.10 $H_f$ (about quarter the embedded depth, $D$) and 0.20 $H_f$ (about half the embedded depth, $D$), from the dredge line, for low and high wall stiffness, respectively. Formulas to evaluate the maximum lateral movement, bending moment of the wall, passive earth pressure and the maximum tensile force within the anchor tie under vertical and horizontal loads due to different design parameters of the anchored sheet pile marine walls are estimated and presented.

## Notations

| | |
|---|---|
| $A$ | is the anchor cross-sectional area, |
| $As$ | is the a constant for either, horizontal or vertical, members |
| $B$ | is the wall width, |
| $c$ | is the soil cohesion, |
| $C$ | is the a factor dependent on the settlement, |
| $c_i$ | is the cohesion at depth $z_i$, |
| $D$ | is the penetration depth, |
| $E$ | is the anchor modulus of elasticity, |
| $E_sI$ | is the sheet pile wall stiffness, |
| $F_{max}$ | is the maximum anchor tensile force, |
| $Bs$ | is the a coefficient for depth, |
| $D/H_f$ | is the penetration Depth ratio, |

$h_a/ H_f$ is the anchor Location ratio,
$h_w/H_f$ is the water Height ratio,
$H_f$ is the free height of wall,
$K_{ae}$ is the anchor equivalent stiffness,
$k_{ai}$ is the active earth pressure coefficient at depth $z_i$;,
$k_{an}$ is the anchor stiffness,
$k_{pi}$ is the passive earth pressure coefficient at depth $z_i$;,
$k_a$ is the active lateral earth pressure coefficient,
$k_s$ is the modulus of sub-grade reaction,
$k_p$ is the passive lateral earth pressure coefficient,
$K_w$ is the sheet pile wall stiffness,
$L$ is the anchor length,
$n$ is the an exponent to give $k_s$ the best fit,
$N_c$, $N_g$, and $N_\gamma$ is are Terzaghi's bearing capacity factors of the soil,
$M_{max}$ is the maximum bending moment,
$p_{pmax}$ is the maximum passive earth Pressure,
$p_h$, is the horizontal Load,
$p_v$ is the vertical applied Load,
$p_a$ is the active earth pressure,
$p_p$ is the passive earth pressure,
$u_i$ is the pore water pressure at depth $I$,
$u$ is the pore water pressure,
$Z$ is the depth of interest below ground,
$q_{ult}$ is the ultimate bearing capacity of the soil,
$\Delta/H_f$ is the lateral movement ratio,
$(\Delta/H_f)_{max}$ is the maximum lateral movement ratio,
$\beta$ is the anchor inclination with the horizontal,
$\delta$ is the wall-soil angle of friction,
$\phi$ is the angle of backfill soil friction,
$\gamma$ is the unit weight of soil,
$\Delta$ is the soil deflection,
$\gamma_d$ is the dry unit weight,
$\gamma_{sub}$ is the submerged unit weight, and
$\Delta_{max}$ is the maximum wall deflection.

## References


[1] J.W. Pappin, B. Simpson, P.J. Felton, and C. Raison, "Numerical Analysis of Flexible Retaining Walls", Proceedings of Symposium on Computer Application in Geotechnical Engineering (1986).

[2] H.H. Vaziri, "Theory and Application of an Efficient Computer Program for Analysis of Flexible Earth-Retaining Structures", International Journal of Computers and Structures, Vol. 56 (1), pp. 177-187 (1995).

[3] H.H. Vaziri, "Numerical Study of Parameters influencing the Response of Flexible Retaining Walls", Canadian Geotechnical Engineering Journal, Vol. 33, pp. 290-308 (1996).

[4] J.E. Bowles, Analytical and Computer Methods in Foundation Engineering, McGraw-Hill Book Co., NY (1974a).

[5] Tschebotarioff, G.P., Large Scale Earth Pressure Tests with Model Flexible Bulkheads, Final Report to Bureau of Yards and Docks U.S. Navy, Princeton University, U.S.A. (1949).

[6] P.W. Rowe, "Anchored Sheet Pile Walls", PICE, Vol. 1 (1), pp. 27-72 (1952).

[7] K. Terzaghi, Special Footings and Beams on Elastic Foundations, Foundation Analysis and Design, McGraw-Hill Book Co., NY, pp. 380-432 (1988).

[8] J.E. Bowles, "Elastic Foundation Settlements on Sand Deposits", JGED, ASCE, Vol. 113 (8), pp. 846-860, (1987).


Received 27 December, 2004
Accepted January 20, 2005